Sub-barrier Coulomb Excitation of ^{110}Sn and its Implications for the ^{100}Sn Shell-closure

J. Cederkäll,[1,2] A. Ekström,[2] C. Fahlander,[2] A. M. Hurst,[3] M. Hjorth-Jensen,[4] F. Ames,[5] A. Banu,[6,7] P. A. Butler,[3] T. Davinson,[8] U. Datta Pramanik,[9] J. Eberth,[10] S. Franchoo,[11] G. Georgiev,[1] M. Górska,[6] D. Habs,[12] M. Huyse,[13] O. Ivanov,[13] J. Iwanicki,[14] O. Kester,[6] U. Köster,[1] B. A. Marsh,[15,16] O. Niedermaier,[17] T. Nilsson,[18] P. Reiter,[10] H. Scheit,[17] D. Schwalm,[17] T. Sieber,[17] G. Sletten,[19] I. Stefanescu,[13] J. Van de Walle,[13] F. Wenander,[16] P. Van Duppen,[13] N. Warr,[10] and D. Weisshaar[10]

[1] *PH Department, CERN 1211, Geneva 23, Switzerland*
[2] *Physics Department, University of Lund, Sweden*
[3] *Oliver Lodge Laboratory, University of Liverpool, United Kingdom*
[4] *Physics Department and Center of Mathematics for Applications, University of Oslo, Norway*
[5] *TRIUMF, Vancouver, Canada*
[6] *Gesellschaft für Schwerionenforschung, Darmstadt, Germany*
[7] *Institut for Nuclear Physics, University of Mainz, Germany*
[8] *Department of Physics and Astronomy, University of Edingburgh, United Kingdom*
[9] *Saha Institute of Nuclear Physics, Kolkata 700064, India*
[10] *Institute of Nuclear Physics, University of Cologne, Germany*
[11] *IPN Orsay, Orsay, France*
[12] *Physics Department, Ludwig-Maximilian University, Munich, Germany*
[13] *Instituut voor Kern- en Stralingsfysica, K.U. Leuven, Belgium*
[14] *Heavy Ion Laboratory, Warsaw University, Poland*
[15] *Department of Physics, University of Manchester, United Kingdom*
[16] *AB Department, CERN 1211, Geneva 23, Switzerland*
[17] *Max-Planck Institute of Nuclear Physics, Heidelberg, Germany*
[18] *Fundamental Physics, Chalmers University of Technology, Gothenburg, Sweden*
[19] *Physics Department, University of Copenhagen, Denmark*

(Dated: March 22, 2007)

The first excited 2^+ state of the unstable isotope ^{110}Sn has been studied in safe Coulomb excitation at 2.82 MeV/u using the MINIBALL array at the REX-ISOLDE post-accelerator at CERN. This is the first measurement of the reduced transition probability of this state using this method for a neutron deficient Sn isotope. The strength of the approach lies in the excellent peak-to-background ratio that is achieved. The extracted reduced transition probability, B(E2:$0^+ \rightarrow 2^+$) = 0.220 $\pm$ 0.022 e^2b^2, strengthens the observation of the evolution of the B(E2) values of neutron deficient Sn-isotopes that was observed recently in intermediate energy Coulomb excitation of ^{108}Sn. It implies that the trend of these reduced transition probabilities in the even-even Sn-isotopes is not symmetric with respect to the mid-shell mass number, $A = 116$, as ^{100}Sn is approached.

PACS numbers: 21.60.Cs 23.20.-g 23.20.Js 23.40.Hc 25.70.De

A substantial interest has been shown recently in the shell-structure of atomic nuclei with only a few nucleons outside the double shell closure at ^{100}Sn. As an example, a series of experiments aiming at isotopes in this region has been carried out using fusion-evaporation reactions in the recent past [1]. With the advent of radioactive ion beams these studies are now taken further using sub-barrier and intermediate energy Coulomb excitation [2, 3]. In this paper we present the only sub-barrier or "safe" Coulomb excitation experiment in this region to date. The study of the reduced transition probability – the B(E2) – of the first excited 2^+ state in an even-even nucleus gives a direct handle on the collectivity of that state. It can thus be used to measure systematic changes in the strengths of shell gaps. The general motivation for this kind of study goes back to our incomplete knowledge of the mechanisms that govern shell formation and their implications for the structure of nuclei far from stability. It is well-known that a strong spin–orbit force was introduced into the nuclear shell-model on Fermi's suggestion by Goeppert-Mayer [4] and independently by Haxel, Jensen and Suess [4] to explain the observed shell gaps. However, these papers were substantially predated by the consideration of a nuclear spin–orbit force by Inglis [5] who noted that the relativistic Thomas term which arises as a consequence of the non-commutation of Lorentz transformations, should act also in atomic nuclei. This term, given by the vector product of the velocity and acceleration of the bound nucleon gives rise to nuclear LS coupling, a result which can be derived from the Dirac equation [6]. In this picture the acceleration is proportional to the derivative of the potential experienced by the bound particle, a notion still used in mean-field approaches today. As a consequence the splitting of the shell gaps becomes density dependent and may change with the distribution of nucleons in the nucleus. Thus, already on a more fundamental level, changes in shell-gap structure could occur for ex-

otic neutron-proton combinations. It should be added that the size of the Thomas term appeared too small to account for the splitting suggested by Goeppert-Mayer and in a later paper Inglis conjectured an addition to spin–orbit partner splitting from meson exchange [7]. In a microscopic description of residual forces in the shell model other considerations also become important. In particular, close to a self-conjugate shell closure correlations will arise between neutrons and protons that occupy orbits with the same quantum numbers. An example of this is so-called neutron-proton pairing [8]. Furthermore, as has been discussed by Otsuka et al. [9] one expects a particularly strong interaction between neutrons and protons occupying spin–orbit partner orbits. In this context the so-called monopole drift of single particle energies with respect to mass number becomes important [10]. A main motivation for a study of shell evolution is thus to see if the shell closures that are strong at stability remain so far from stability as the distribution of nucleons changes. This question is particularly interesting in the self-conjugate case. Coulomb excitation of radioactive beams at safe energies is a new and unique tool to address this topic.

The radioactive ^{110}Sn beam used in the experiment was produced by bombarding a 27 g/cm^2 LaC_x target at ISOLDE, CERN, with a 1.4 GeV proton beam from the PS booster. The Sn atoms, after having diffused through the heated target material and effused into an ionization cavity, were ionized by a three-step laser ionization scheme whereafter the beam was extracted and separated in the general purpose separator of the facility. This method provides a high degree of mass and element selectivity. Samples were collected with the laser beams switched on and off to identify the components of the beam. Collection of ^{110}Sn is possible as its half-life is 4.1 h. The γ-rays emitted following β-decay in the sample were measured offline using γ-spectroscopic methods. It was concluded that Sn ions were implanted only when the laser beams were switched on. Furthermore, surface ionized ^{110}In was identified as the main beam contaminant. A yield of $2.5 \cdot 10^8$ atoms/μC of ^{110}Sn was established from this measurement. The yield of ionized contaminant ^{110}In was one order of magnitude smaller. The intensity of the post-accelerated beam was set to $\sim 10^6$ p/s on the secondary target. Due to the high production yield the beam current could be measured using pico-am meters with the lasers switched on and off, respectively. This was done at ten different occasions during the experiment in order to determine possible variations in beam composition. The measurements rendered a beam purity, consistent with the offline measurements, of 90.0± 1.4% . Decay γ-rays as well as Coulomb excitation γ-rays from other contaminants than ^{110}In were searched for in the final data set but were not observed.

As has been discussed previously [11] the REX-ISOLDE post-accelerator relies on charge breeding in an electron beam ion source (EBIS) as a first step. The charge breeder and the preceding beam cooling, accomplished by catching the ion bunch from the separator in a gas-filled Penning trap, set the repetition frequency of the beam. In this case the beam was charge bred to the 27^+ charge state over an EBIS confinement time of 98 ms. The extracted beam pulse had a duration of approximately 100 μs with a decaying exponential time profile. The beam was accelerated to 2.82 MeV/u in the REX-ISOLDE linac before hitting a 2 mg/cm^2 and 99.9% pure ^{58}Ni target. Due to the characteristic inverse kinematics of the experiment, beam and target particles emerge in a significantly forward-focussed cone after scattering. Coulomb excitation experiments at REX-ISOLDE use a setup that measures the energies and angles of emitted γ-rays and scattered charged particles. The secondary target position is surrounded by a set of Ge detectors, in a close geometry, called the MINIBALL array [12]. The Ge detectors run independently using sampling ADCs with a common clock. The setup comprises 24 high-purity Ge crystals with a total of 144 segments. The typical photopeak efficiency is ∼10% at 1.3 MeV. A circular double sided silicon strip detector (DSSSD) is located 30.6 mm downstream of the target. It registers the energy and angle of a scattered beam and/or target particle (see Fig. 1). To

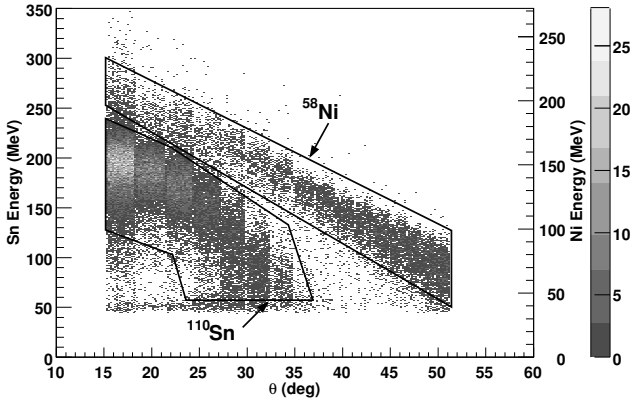

FIG. 1: Scattered beam and target particles as detected in the DSSSD. The upper branch corresponds to scattered ^{58}Ni and the lower branch to ^{110}Sn particles, respectively. The kinematical cuts used for the identification of beam and target particles are also indicated in the figure.

TABLE I: The second and third rows give the intensities for the Doppler corrected Coulomb excitation peaks of ^{58}Ni and ^{110}Sn from the sum of hits per bin with corresponding background subtraction and from fitting a Gaussian with linear background. The last row gives the B(E2;$0^+ \rightarrow 2^+$) in e^2b^2 for ^{110}Sn using these numbers, respectively.

	Energy (keV)	Bin Area	Fitted Area
^{58}Ni	1454.4	237±15	222±15
^{110}Sn	1211.9	579±24	588±24
B(E2) e^2b^2		0.220±0.022	0.238±0.024

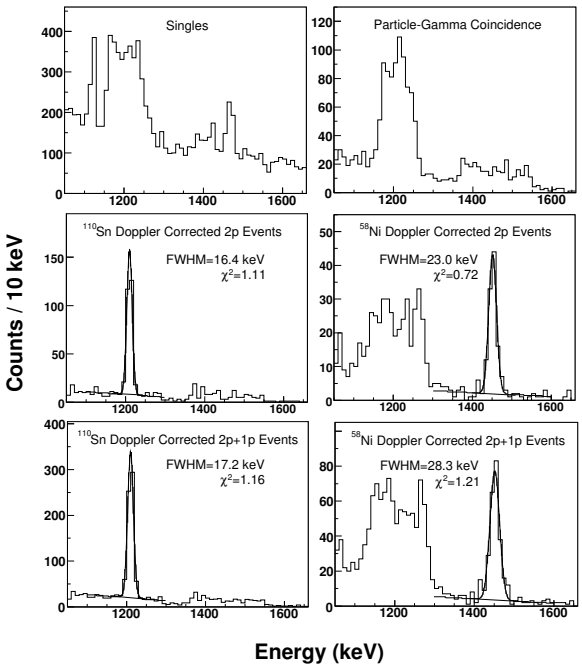

FIG. 2: Single and particle-γ coincindence γ-ray spectra before Doppler correction (top panels). Doppler-corrected γ-ray spectra for 2-particle γ-ray coincident events (central panel) and the corresponding Doppler corrected γ-ray spectra for the sum of 2-particle and 1-particle reconstructed events for ^{110}Sn and ^{58}Ni (bottom panel). See text for detailed discussion.

remedy possible dead-time effects the trigger for the particle detector included a raw particle trigger downscaled a factor of 2^6, and a γ-ray and charged particle coincidence trigger. The DSSSD comprises 16 annular (front face) and 24 radial (back face) strips. It is subdivided into four separate quadrants. The combined segmentation of the Ge detectors and the DSSSD makes it possible to reconstruct the kinematics of individual Coulomb excitation events for Doppler correction. At 2.82 MeV/u the incoming beam travels at $\beta\sim8\%$ which results in a complete broadening of the raw γ-ray spectrum. The effect can be seen in Fig. 2.

In this experiment we selected the beam and target such that the kinematical difference in angle and energy of the two can be used for particle identification (Fig. 1). The scattered beam reaches its maximum scattering angle at $\sim$31.8° and scattered target particles at $\sim$84.1°. All angles in this experiment correspond to safe collisions, i.e. there is no inter-nuclear overlap. One can also note that the multiple-step excitation probability, or the probability to excite any other state than the first 2^+ is negligible with this choice of kinematics. Two features of Fig. 1. can be commented on. First, the energy used for Doppler correction was calibrated using energy loss simulations and the known maximum scattering angle for ^{110}Sn. The main effect of this improved calibration is to reduce the half-width of the Doppler-corrected γ-ray peaks. Second, the broadening of the Sn and Ni branches in Fig. 1. is almost entirely caused by differences in emission angle due to the finite size of the beam spot. The two-body kinematics of the experiment was such that every Ni ion scattered within the angular range of the DSSSD is coincident with a beam particle scattered between 24° and 31.8°. Thus a substantial part of the dataset contains 2-particle+γ-ray (2p+γ) coincidences. This is advantageous as it gives a direct correlation between the number of scattered ^{110}Sn ions, ^{58}Ni ions and emitted γ-rays. It also provides for Doppler correction for both particles using the energy detected in the DSSSD. The Doppler corrected spectra for these events are shown in the central panel of Fig. 2. A sub-set of events contains only 1-particle + γ-coincidences (1p+γ). These correspond either to the range for scattered beam below 24° or to events where only one hit could be uniquely reconstructed from the DSSSD. This is e.g. due to noise or double hits. Note that in a true 2p event the particles come back-to-back in the CM-system and are thus detected in opposite quadrants in the DSSSD and cannot cause double hits. Furthermore, two-body kinematics can be completely reconstructed by detecting one of the particles. As seen in Fig. 2 reconstruction leads to a slightly larger half-width. The intensities obtained in this fashion were used to extract the B(E2) for the first 2^+ state in ^{110}Sn. The method relies on the fact that the B(E2) for the first 2^+ state in ^{58}Ni is known. The cross section for exciting target and beam particles is proportional to the corresponding B(E2). The angular distribution of the cross-section was calculated for the relevant angular ranges using the code CLX [13]. Taking into account the beam purity, a small angular correction and the γ-ray detection efficiency, the B(E2) for the first 2^+ state in ^{110}Sn was determined to be B(E2)= 0.220 ± 0.022 e^2b^2 (see Table 1). The method and the proof-of-principle have been described in Refs. [14, 15]. The new result (see Fig. 3) corroborates the published result from intermediate-energy Coulomb excitation of ^{108}Sn [2]. The two results imply that the first 2^+ states in the even-even neutron deficient Sn isotopes retain a relatively large part of collectivity compared to the neutron rich isotopes. These states have a constant energy of $\sim$ 1200 keV which has been explained from the seniority scheme. We note that a recent safe Coulomb excitation measurement for ^{114}Sn at GSI has reduced the error bar of the B(E2) for that 2^+ state to same range as for ^{116}Sn but that a shift towards a higher B(E2) remains [16]. In the following we compare the measured B(E2) value in ^{110}Sn to the results of two large-scale shell model calculations (see Ref.[2]). As a starting point note that the $1d_{5/2}$ and $0g_{7/2}$ orbits are neutron valence orbits from ^{114}Sn towards ^{100}Sn. The main proton valence orbit is $0g_{9/2}$. The calculations, carried out by the Oslo and Strasbourg groups, used effective interactions defined for two different cores, namely ^{100}Sn and ^{90}Zr, but using the same nucleon-nucleon interaction. Details on how to derive the

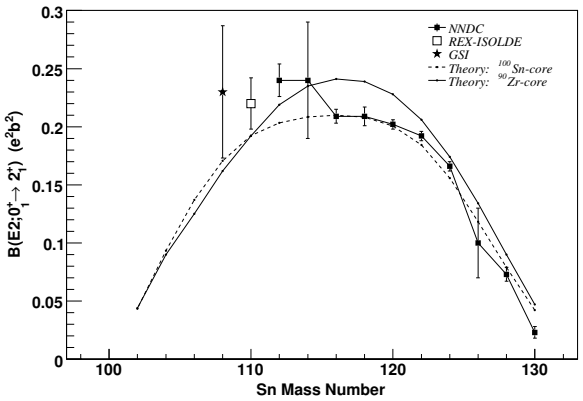

FIG. 3: Current status of measured B(E2) values for the first 2^+ state in even-even Sn isotopes. Note the shift in B(E2) in ^{114}Sn as the $g_{7/2}$ and $d_{5/2}$ orbits start to dominate the configuration. The χ^2, taken per degree of freedom, for the deviation between the experimental values and the theoretical predications for the mass number sequences A_1={114,112,110,108}, A_2={114,112,108} and A_3={114,112,110} is χ^2_1=1.6, χ^2_2=1.7 and χ^2_3=1.9 for the ^{90}Zr core. The corresponding values for the ^{100}Sn core is χ^2_1=3.3, χ^2_2=4.2 and χ^2_3=4.4, respectively. Consequently due to the rather small error the current measurement is statistically a more significant test of the deviation from theory than the previous measurement of ^{108}Sn.

effective interactions are given in [17]. The ^{90}Zr case includes protons in the $1d_{5/2}$, $0g_{7/2}$, $0g_{9/2}$, $1d_{3/2}$ and $2s_{1/2}$ and neutrons in the $1d_{5/2}$, $0g_{7/2}$, $1d_{3/2}$, $2s_{1/2}$ and $0h_{11/2}$ single-particle orbits. For a ^{100}Sn core, neutrons confined to the $1d_{5/2}$, $0g_{7/2}$, $1d_{3/2}$, $2s_{1/2}$ and $0h_{11/2}$ single-particle orbits define the shell-model space. In the calculation of the B(E2) systematics, an effective neutron charge of $0.5e$ and proton charge $1.5e$ were used for the ^{90}Zr core while an effective neutron charge of $1.0e$ was used for the ^{100}Sn case. The results are displayed in Fig. 3. In the case of a ^{100}Sn core, the experimental B(E2) values are reproduced for all isotopes down to ^{116}Sn. Starting with ^{114}Sn, the theoretical results display the expected parabolic behavior but are at askance with the experimental result for ^{110}Sn and the result for ^{108}Sn [2]. Similar results have emerged for ^{110,108,106}Sn [3] from intermediate-energy experiments during the preparation of this paper. To reproduce the experimental values one needs a larger effective charge. Furthermore, the experimental values seem to deviate from a good seniority picture for the lighter Sn isotopes. The transition rates are almost independent of the mass number A. Thus the effective charges for the lighter Sn isotopes show stronger renormalization effects. This implies larger core polarization due to particle-hole excitations, and a different character of core excitations in the $N = Z$ and $N \gg Z$ regions of the Sn isotopic chain. To further investigate the variation and intrinsic *ph* structure of the polarization charge in the pure neutron space, Ref. [2] included a calculation with ^{90}Zr as core with up to four-particle-four-hole proton excitations (current computational limit). In this way one can reproduce the same trend as for the ^{100}Sn core but with an effective charge for neutrons of $0.5e$ and protons of $1.5e$. These non-renormalized charges are discussed by e.g. Bohr and Mottelson [18]. However, still the enlarged calculations deviate from the new experimental data for lighter Sn isotopes. We note that the current result indicates that further core-polarization effects may be needed and/or a better effective interaction introduced. Here the proton-neutron interaction plays an essential role. In particular the $\pi(0g_{9/2})-\nu(0g_{7/2}1d_{5/2}1d_{3/2}2s_{1/2})$ monopoles, responsible for the evolution of the spectroscopy between ^{91}Zr and ^{101}Sn, govern the evolution of the proton $Z = 50$ gap with the neutron filling. These monopoles were fitted to reproduce the experimental spectra of nuclei around $A \sim 100$. Here the $\pi(0g_{9/2})-\nu(1h_{11/2})$ monopole in particular suffer from experimental uncertainties. In conclusion, we note the present experimental result, using safe energy Coulomb excitation deviates from current theoretical descriptions of the Z=50 shell gap. Further experiments investigating the reduced transition probability of the corresponding states in lighter even-even Sn isotopes are clearly of importance to further illuminate this question. This work was supported by the European Union through RII3-EURONS (contract no. 506065).

[1] M. Gorska *et al.* Phys. Rev. Lett. **79**, 2415 (1997); M. Lipoglavsek *et al.* Physics Lett. **B440**, 246 (1998)
[2] A. Banu *et al.* Phys. Rev. C **72**, 061305 (R) (2005)
[3] C. Vaman *et al.* e-Print Archive: nucl-ex/0612011.
[4] M.G. Mayer, Phys. Rev. **75**, 1969 (1949); O. Haxel, J. H. D. Jensen and H. E. Suess, Phys. Rev. **75**, 1766 (1949).
[5] D. R. Inglis, Phys. Rev. **50**, 783 (1936); S. Dancoff and D. R. Inglis, Phys. Rev. **50**, 784 (1936).
[6] W. H. Furry, Phys. Rev. **50**, 784 (1936).
[7] D. R. Inglis, Phys. Rev. **75**, 1767 (1949).
[8] A. L. Goodman, Adv. Nucl. Phys. **11**, 263 (1979)
[9] T. Otsuka *et al.* Phys. Rev. Lett. **87**, 082502 (2001).
[10] P. Federman and S. Pittel, Phys. Rev. C**20**, 820 (1979)
[11] D. Habs *et al.* Nuclear Instrum. and Methods **B139**, 128 (1998)
[12] P. Reiter *et al.* Nuclear Phys. **A701**, 209 (2002)
[13] H. Ower, Computer program CLX.
[14] O. Niedermaier *et al.* Phys. Rev. Lett **94**, 172501 (2005) and references therein.
[15] A. M. Hurst *et al.* Phys. Rev. Lett **98**, 072501 (2007)
[16] P. Doornenbal *et al.* to be published.
[17] M. Hjorth-Jensen, T. T. S. Kuo, and E. Osnes, Phys. Rep: **261**, 125 (1995).
[18] Aa. Bohr and B. Mottelson, *Nuclear Structure*, (W. A. Benjamin, New York, 1969), Vol. 1.